Publication Date: 10 March 2024
Archs Sci. (2024) Volume 74, Issue 1 Pages 81-85, Paper ID 2024110.
https://doi.org/10.62227/as/74110

A study of $^{16}O +^{166} ER$, $^{16}O+^{197}$Au Systems using Calculations of Quasi-elastic Scattering

Ali A. Rakhees[1,*] and Khalid S. Jassim[1]
[1]Department of Physics, College of Education for pure Science, University of Babylon, Hilla-Babylon, Iraq.
Corresponding authors: Ali A. Rakhees (e-mail: ali.rakhees.pure396@student.uobabylon.edu.iq).

Abstract Specific systematic studies on the nuclear potential parameter for the heavy-ion reactions which includes the systems have been achieved by using large-angle quasi elastic scattering at deep sub-barrier energies close to the Coulomb barrier height. The elastic scattering barrier distribution D_{qel}as a function of energy has also been calculated in this theoretical study. The single-channel (SC) and coupled-channels calculations have been carried out to elicit the nuclear potential. The chi-square method X^2 has been used find the best value of the nuclear potential in comparison with the experimental data. The best values of the nuclear potential were found from the calculations of the single channels for systems: $^{16}O +^{166} ER$, $^{16}O+^{197}$Au, which are equal to (60.5, 100) MeV, respectively.

Index Terms Quasi-elastic scattering, Woods Saxon potential, nuclear potential parameter

I. Introduction

The Coulomb barrier region offers a highly broad range of events in heavy ion collisions. The barrier splits as a result of different channels interfacing with one another [1], consequently, when compared to one-dimensional calculations, greatly raises the fusion cross sections in the sub-barrier region [2]. In nuclear physics, the tunneling phenomenon is shown by the fusion of two nuclei at extremely low energy. These processes not only play a crucial role in the synthesis of nucleic nucleosynthesis, and the creation of stellar energy, but they also shed fresh light on nuclear structure and reaction dynamics [3]. Heavy-ion fusion cross-sections may be replicated using a barrier penetration model at energy far higher than the Coulomb barrier. Combining the attractive short-range nuclear potential with the repulsive Coulomb and centrifugal potentials results in the one-dimensional fusion barrier [4].

Measured fusion cross-sections are commonly increased by calculations performed with this model for energy below this single barrier. It has long been understood and experimentally proven that static deformation effects can improve sub-barrier fusion. In this case, the amplification is caused by the dispersion of barrier heights, which may be understood as the result of different target nuclei's distorted orientations [5]. Since penetration through the single barrier is substantially less likely than going over the smaller obstacles, the cross sections are boosted by any distribution of barriers around the single barrier, at energies lower than that of the single barrier [6].

A semi-classical model was used to examine the impact of surface vibrations collectively on fusion, which once more led to the dispersion of fusion barriers, even though crossing barriers whose heights are often lower than the fusion energy is what causes the majority of the cross sections [7]. The connection between separate reaction channels results in a dispersion of barriers instead of a single barrier [8]. The fusion barrier distribution, which incorporates the second derivative, may be used to conveniently study the sensitivity of fusion data to the coupling of distinct reaction channels. Furthermore, the potential parameters employed in theoretical calculations may be restricted by selecting a set of parameters that can duplicate the barrier distribution as precisely as feasible [9]. To get an accurate barrier distribution, very precise fusion cross sections must be measured [10].

Larger mistakes in the distribution extraction occur at energies slightly over the barrier when using the second derivative to derive the distribution. As an alternative, it was suggested that backward-angle quasi-elastic (QEL) scattering may produce a comparable distribution [11]. In general, scattering studies with heavy ions accelerated to varying energies and conducted on a variety of fixed targets have proven to be an helpful tool for learning more about the specifics of the interaction processes at as well as the characteristics of the nucleus itself, as demonstrated by the Geiger and Marsden experiments [12]. As a consequence, All interactions entail essentially the same information regarding the interaction mechanism and are subject to the same potential, both of which are vulnerable to channel coupling effects at energies near the colliding nucleus [13].

ARCHIVES DES SCIENCES
A Multidisciplinary Journal

The couplings between motion and internal degrees of freedom in the colliding nuclei are primarily responsible for heavy-ion reactions at energies close to and below the Coulomb barrier [14]. One famous example is the rise in the sub-barrier fusion cross-sections relative to basic potential model predictions, which is attributed to strong couplings to mutual excitement [13]. For a number of heavy-ion systems, coupled-channel studies have been offered, accounting for particular coupling effects that fully explain quasi-elastic back angle scattering and experimental fusion interaction evidence [15]. The of this study is to obtain the nuclear potential parameters for the systems $^{16}O+^{166}ER$, $^{16}O+^{197}$Au by using large angle quasi-elastic scattering at deep sub-barrier energies close to the Coulomb barrier height, and the single channels and coupled-channels calculations were performed using the CQEL program, which includes all orders of coupling and is considered the most recent version of computer code CCFULL [16]. The best fitted values of the nuclear potential parameters in comparison with the experimental data have been obtained through the chi square method X^2 [16]. Jassim and et al. have been studied quasi-elastic scattering for some heavy ion systems to find diffuseness parameters and some others important parameters [17]–[21].

II. Theory

Using the coupled channels technique, the nuclear structural impacts may be considered in a more quantal manner. To develop the coupled channels approach, consider a collision between two nuclei in the presence of the coupling of the relative motion $r = (r, \hat{r})$ to a nuclear intrinsic motion ξ. We assume the following Hamiltonian for this system [17], [22]:

$$H\left(\vec{r},\xi\right) = \frac{\mathrm{h}^2}{2\mu}\nabla^2 + V\left(r\right) + H_0\left(\xi\right) + V_{coup}\left(\vec{r},\xi\right), \quad (1)$$

where $H_o(\xi)$ and $V_{coup}(r.\xi)$, are the intrinsic and the coupling Hamiltonians, respectively and $V(r)$ is the standard Woods-Saxon potential which has the form [17]:

$$V_N\left(r\right) = -\frac{V_0}{1+\exp\left[\frac{r-R_0}{a}\right]}, \quad (2)$$

where a represents the diffuseness parameter. In general, the fundamental degree of freedom ξ has limited spin. Consequently, we raise the multipole coupling Hamiltonian [19]:

$$V_{coup}\left(\vec{r},\xi\right) = \sum_{\lambda>0,\mu} f_\lambda\left(r\right)\ Y_{\lambda\mu}(\hat{r})\, T_{\lambda\mu}(\xi). \quad (3)$$

Here $Y_{\lambda\mu}(\hat{r})$ are the spherical harmonics and $T_{\lambda\mu}(\xi)$ are spherical tensors built using the intrinsic coordinate system. The dot indicates a scalar product. The sum is taken over all except for λ = 0, this is already present in the bare potential, V(r). For a fixed total angular momentum J and its z-component M, the wave function's expansion basis in Eq. (2) is described as [19].

$$\left\langle \vec{r}\,\xi \,\middle|\, (nlI) \,\middle|\, JM \right\rangle = \sum_{m_l m_I} \langle lm_l I m_I \mid JM\rangle Y_{lm_l}\left(\hat{r}\right)\ \varphi_{n_I m_I}\left(\xi\right). \quad (4)$$

The intrinsic motion wave functions are subject to where $\varphi_{n_I m_I}(\xi)$ are the wave functions I; l are the intrinsic and orbital angular momenta, respectively [17], [23]:

$$H_0\left(\xi\right)\ \varphi_{n_I m_I}\left(\xi\right) = \epsilon_n \varphi_{n_I m_I}\ \left(\xi\right). \quad (5)$$

In this context, stands for any quantum number beside angular momentum α. Using the channel wave functions, the overall wave function is amplified as [19]:

$$\psi\left(\vec{r},\xi\right) = \sum_{n,l,I} \frac{u^J_{nlI}\left(r\right)}{r}\ \langle \vec{r}\xi \mid (nlI) \mid JM\rangle. \quad (6)$$

The equations for $u^J_{nlI}(r)$ in the coupled channels are as follows [19], [23]:

$$\left[-\frac{\mathrm{h}^2}{2\mu}\frac{d^2}{dr^2} + V\left(r\right) + E + \epsilon_n\right] u^J_{nlI}\left(r\right) + \sum_{n'l'I'} V^J_{nlJ;n'l'I'}\left(r\right) u^J_{n'l'I'}\left(r\right) = 0. \quad (7)$$

In which the elements of the coupling matrix $V^J_{nlJ;n'l'I'}(r)$ are defined as [17]:

$$V^J_{nlJ;n'l'I'}\ (r) = \left\langle JM\left(nlI\right) \,\middle|\, V_{coup}\left(\vec{r},\xi\right) \,\middle|\, \left(n'l'I'\right) JM\right\rangle;$$

$$V^J_{nlJ;n'l'I'}\ (r) = \sum_\lambda (-1)^{I-I'+l'+\mathrm{J}} f_\lambda\left(r\right) \left\langle l \,\|Y_\lambda\|\, l'\right\rangle \times \langle nI \,\|T_\lambda\|\, n'I'\rangle \times \sqrt{(2l+1)(2I+1)} \begin{Bmatrix} I' & l' & J \\ l & I & \lambda \end{Bmatrix}$$

Since the coefficient is independent of the coefficient M., as can be seen in the equation, it has been suppressed, and suppres the index J. After that, linked channels Eq. (7) reads as [17], [19]:

$$\left[-\frac{\mathrm{h}^2}{2\mu}\frac{d^2}{dr^2} + V\left(r\right) + E + \epsilon_n\right] u^J_{nlI}\left(r\right) + \sum_{n'l'I'} V^J_{nlJ;n'l'I'}\left(r\right) u^J_{n'l'I'}\left(r\right) = 0. \quad (8)$$

We may define the wave number, k_n(r), by:

$$k_n\left(r\right) = \sqrt{\frac{2\mu}{\mathrm{h}^2}\ \left(\begin{array}{c} E\ -\epsilon_{nI}\ -\frac{\mathrm{h}^2}{2\mu r^2}\ -\ V\left(r\right) - \\ v^J_{nlI;nlI}\left(r\right) \end{array}\right)}, \quad (9)$$

where

$$k_n = \sqrt{\frac{2\mu\left(E\ -\ \epsilon_n\right)}{\mathrm{h}^2}}. \quad (10)$$

With that, we calculate the fusion cross section by [17]:

$$\sigma_{fus}\left(E\right) = \frac{\pi}{K^2}\sum_J \left(2J+1\right) P^J\left(E\right). \quad (11)$$

The distribution of fusion barriers is calculated by [17]:

$$D_f\left(E\right) = \frac{d^2(E\sigma_{fus})}{dE^2} = \pi R_b^2 \left[-\frac{d}{dE}\left[\frac{1}{1+\exp\left[2\pi\frac{E-V_b}{h^2\omega}\right]}\right]\right].$$

ARCHIVES DES SCIENCES
A Multidisciplinary Journal

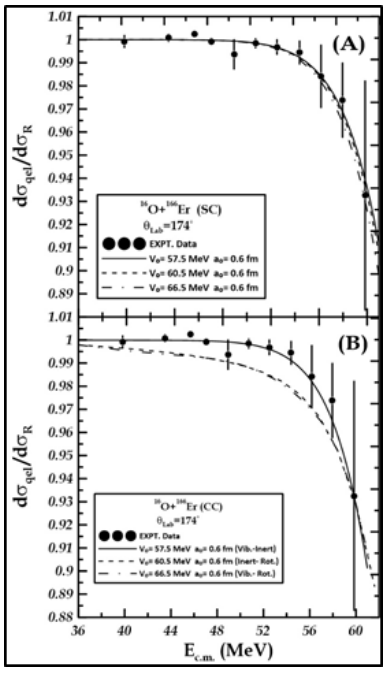

Figure 1: Calculations for single and coupled-channel ($^{16}O+^{166}ER$) systems: Panels (A);(B) display the cross-sections of quasi-elastic scattering with a mass center to energy, whereas panels (C);(D) Present the distribution of the quasi-elastic scattering barrier using a mass center to energy; the experimental findings are presented in the black circles

III. Results and Discussion

In $^{16}O+^{166}ER$ system, We determined the nuclear potential parameter under conditions where both the projectile ^{16}O and the target ^{166}Er were considered to be single channel (SC) inert nuclei; as shown in Figure 1, with the nuclear potential's parameter values V_o= (57.5,60.5,66.5) MeV respectively. In yet another instance, we assumed vibrational projectile ^{16}O using a parameter for deformation β_o=0.358 to the a state 2^+(6.917MeV) [24], with inert nucleus ^{166}Er, parameter value of the nuclear potential V_o=57.5MeV, the diffuseness a_o =0.6fm. In another case, the projectile ^{16}O we suppose as inert nuclei, and considered target ^{166}Er as rotational nucleus ; and a deformation a parameter β_2=0.285 and β_4= 0.007 [24], using a parameter's diffuseness value a_o = 0.6fm, the nuclear potential V_o =60.5MeV , and the last event, we considered the target ^{166}Er nucleus as nuclei of a rotational coupled with the projectile as vibrational nuclei ^{16}O using a parameter for deformation β_o=0.358 to the state 2^+(6.917MeV), value of the nuclear potential V_o= 66.5MeV , the radius parameter r_o=1.2fm and $\theta_{Lab.} = 174°$.

For $^{16}O+^{166}ER$ system, the better-fitted nuclear potential parameter taken by measuring single channels is 60.5MeV, with X^2 = 0.00001and a_o = 0.6fm. The dashed curve in (Figure 1) shows this. the good-match nuclear potential parameter, observed through a single-channel analysis, makes the experimental data a better fit than the one produced from a coupled channel analysis.

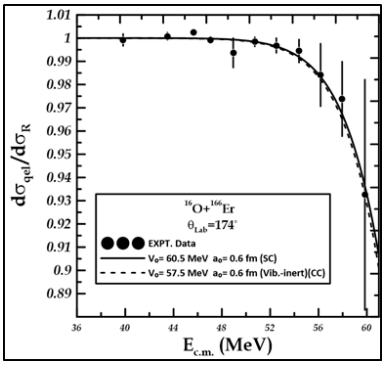

Figure 2: Comparison of the optimal coupling channel value vs the optimal single channel value

A comparison of the optimal values for the single channel and coupling channel, as determined by the chi-square X^2 code, is shown in (Figure 2).

In $^{16}O+^{197}$Au system, we determined the nuclear potential parameter under conditions where both the projectile ^{16}O and the target ^{197}Au were considered to be single channel (SC) inert nuclei; as shown in (Figure 3), with the nuclear potential's parameter values V_o= (100,115,125) MeV respectively. In yet another instance, we assumed vibrational projectile ^{16}O with a deformation a parameter β_o=0.358 to the a state 2^+(6.917MeV)[24], with inert nucleus ^{197}Au, parameter value of the nuclear a potential in this state V_o=100MeV, the diffuseness a_o=0.63fm. in the another case, the projectile ^{16}O suppose as inert nuclei and considered target ^{197}Au to be a rotational nucleus; and to have a deformation a parameter β_2 = -0.125 and β_4=-0.017[24], using a parameter's diffuseness value a_o = 0.63fm, the nuclear potential V_o = 115MeV , and the last event; we considered the target ^{197}Au nucleus as a rotational coupling with the projectile as vibrational nuclei ^{16}O value of the nuclear potential V_o=125MeV, the radius parameter r_o=1.2fm and $\theta_{Lab.} = 174°$.

For $^{16}O+^{197}$Au system, the better-fitted nuclear potential parameter taken by measuring single-channels is 100MeV, with X^2=0.00001and a_o = 0.63fm. the solid curve in Figure 3 shows this. the good-match nuclear potential parameter, observed through a single-channel analysis, renders a better match for the experimental data than the result of a coupled-channel analysis.

A comparison of the optimal values for the single channel and coupling channel, as determined by the chi-square X^2 code, is shown in Figure 4.

IV. Conclusion

The method of large angle quasi-elastic scattering at deep sub barrier energies close to the Coulomb barrier height has shown to be a useful tool for examining the surface characteristics of inter-nucleus potential via precise and methodical analysis of the data. We note the correspondence between the theoretical calculations and the practical values in the graphs between the cross-section ($d\sigma_{qel}/d\sigma_R$) and the energy of the

ARCHIVES DES SCIENCES
A Multidisciplinary Journal

System	Case	$r_o(fm)$	$a_o(fm)$	$V_o(MeV)$	$\sigma_{qel}/\sigma R(X^2)$
16O+166Er	Single channel	1.2	0.6	57.5	0.00002
				60.5	0.00001
				66.5	0.00011
	Vib+Inert. Inert+Rot.Vib+Rot.	1.2	0.6	57.5	0.00010
				60.5	0.00012
				66.5	0.00014

Table 1: The parameters a_o,r_o,V_o, and WS potential, as well as X^2 values, are show to fit theoretical and experimental data

System	Case	$r_o(fm)$	$a_o(fm)$	$V_o(MeV)$	$\sigma_{qel}/\sigma R(X^2)$
16O+197Au	Single channel	1.2	0.63	100	0.00001
				115	0.00003
				125	0.00011
	Vib.+Inert. Inert.+Rot. Vib.+Rot.	1.2	0.63	100	0.00002
				115	0.00005
				125	0.00010

Table 2: The parameters a_o,r_o,V_o, and WS potential, as well as X^2 values, are show to fit theoretical and experimental data

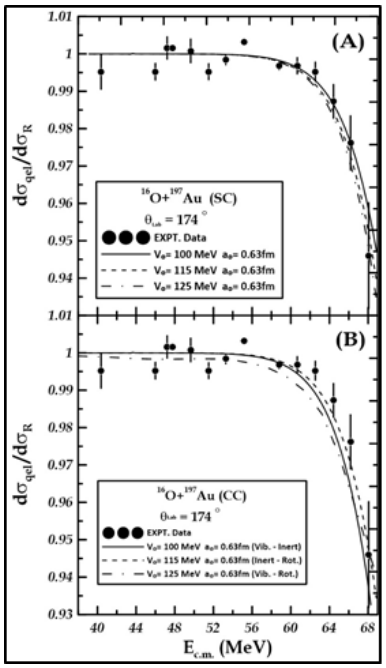

Figure 3: Calculations for single and coupled-channel ($^{16}O+^{197}$Au) systems: Panels (A);(B) display the cross-sections of quasi-elastic scattering with a mass center to energy, whereas panels (C);(D) Present the distribution of the quasi-elastic scattering barrier using a mass center to energy; the experimental findings are presented in the black circles

center of mass. It was found that the best values obtained using the chi-square method are from the single channels. As compared with the rotational coupling, the system's vibration coupling was more successful in simulating experimental data and carrying out theoretical computations. We notice that the correspondence between practical and theoretical values often occurs in the region of low energies, and the cause this is that the region of low energies is under the coulomb potential barrier, which is the region in which the quasi-elastic scattering occurs.

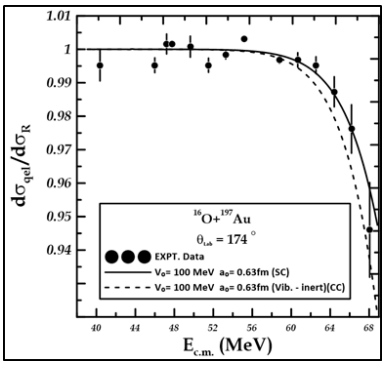

Figure 4: Comparison of the optimal coupling channel value vs the optimal single channel value

References

[1] Timmers, H., Leigh, J. R., Dasgupta, M., Hinde, D. J., Lemmon, R. C., Mein, J. C., ... & Rowley, N. (1995). Probing fusion barrier distributions with quasi-elastic scattering. Nuclear Physics A, 584(1), 190-204.

[2] Kalkal, S., Mandal, S., Madhavan, N., Prasad, E., Verma, S., Jhingan, A., ... & Singh, R. (2010). Channel coupling effects on the fusion excitation functions for Si 28+ Zr 90, 94 in sub-and near-barrier regions. Physical Review C, 81(4), 044610.

[3] Stefanini, A. M., Tivelli, A., Montagnoli, G., Napoli, D. R., Bonamini, D., Beghini, S., ... & Rizzo, F. (1990). Coupled reaction channels effects in the elastic scattering of S 3 2, 3 6+ 5 8, 6 4 Ni. Physical Review C, 41(3), 1018.

[4] Stefanini, A. M., Corradi, L., Vinodkumar, A. M., Feng, Y., Scarlassara, F., Montagnoli, G., ... & Bisogno, M. (2000). Near-barrier fusion of 36 S+ 9 0, 9 6 Zr: The effect of the strong octupole vibration of 96 Zr. Physical Review C, 62(1), 014601.

[5] Hagino, K., & Watanabe, Y. (2007). Potential inversion with sub-barrier fusion data reexamined. Physical Review C, 76(2), 021601.

[6] Naik, R. (2007). Studying fusion reactions for effect of P (CN) on heavy nucleus formation and for nuclear structure effects. Oregon State University.

[7] Piasecki, E., Keeley, N., Kisieliński, M., Kowalczyk, M., Khlebnikov, S., Krogulski, T., ... & Trzcińska, A. (2012). Smoothing of structure in the fusion and quasielastic barrier distributions for the 20 ne+ 208 pb system. Physical Review C, 85(5), 054608.

[8] Leigh, J. R., Dasgupta, M., Hinde, D. J., Mein, J. C., Morton, C. R., Lemmon, R. C., ... & Rowley, N. (1995). Barrier distributions from the fusion of oxygen ions with Sm 1 4 4, 1 4 8, 1 5 4 and W 186. Physical Review C, 52(6), 3151.

[9] Lozano, M., & Madurga, G. (1980). Exponential optical potentials for heavy-ion elastic scattering. Nuclear Physics A, 334(2), 349-364.

[10] Monteiro, D. D. S., Shorto, J. M. B., Huíza, J. F. P., Gomes, P. R. S., & Crema, E. (2007). Derivation of the surface diffuseness of the nucleus-

nucleus interaction potential using large-angle quasielastic scattering at deep sub-barrier energies. Physical Review C, 76(2), 027601.

[11] Silva, C. P., Alvarez, M. A. G., Chamon, L. C., Pereira, D., Rao, M. N., Rossi Jr, E. S., ... & Santra, S. (2001). The heavy-ion nuclear potential: determination of a systematic behavior at the region of surface interaction distances. Nuclear Physics A, 679(3-4), 287-303.

[12] Rowley, N. (2012, September). Geiger-Marsden experiments: 100 years on. In Journal of Physics: Conference Series (Vol. 381, No. 1, p. 012086). IOP Publishing.

[13] Lemasson, A., Shrivastava, A., Navin, A., Rejmund, M., Keeley, N., Zelevinsky, V., ... & Schmitt, C. (2009). Modern Rutherford experiment: Tunneling of the most neutron-rich nucleus. Physical Review Letters, 103(23), 232701.

[14] Keeley, N., Raabe, R., Alamanos, N., & Sida, J. L. (2007). Fusion and direct reactions of halo nuclei at energies around the Coulomb barrier. Progress in Particle and Nuclear Physics, 59(2), 579-630.

[15] Balantekin, A. B., & Takigawa, N. (1998). Quantum tunneling in nuclear fusion. Reviews of Modern Physics, 70(1), 77.

[16] Hagino, K., Rowley, N.,& Kruppa, A. T. (1999). A program for coupled-channel calculations with all order couplings for heavy-ion fusion reactions. Computer Physics Communications, 123(1-3), 143-152.

[17] Majeed, F. A., Jassim, K. S., & Abbas, N. H. Role of Coupled-Channels in Heavy Ions Reactions at the Coulomb Barrier. System, 5, 2.

[18] Hayef, N. H., & Jassim, K. S. (2021). Effect of Surface Diffuseness Parameter on Quasi-elastic Scattering Calculations for 16O+ 208Pb, 63Cu Systems. NeuroQuantology, 19(10), 100.

[19] Rakhees, A. A., & Jassim, K. S. (2023). A Study the Nuclear Potential Using Quasi-Elastic Scattering Calculation for the 9, 10, 11Be+ 208Pb Reactions. East European Journal of Physics, (3), 198-206.

[20] Hamood, F. J., & Jassim, K. S. (2023). The influence changing of Nuclear Potential on Quasi-Elastic Scattering in 16O+ 160Gd and 12C+ 197Au Systems. East European Journal of Physics, (3), 192-197.

[21] Hayef, N. H., & Jassim, K. S. (2023, February). Coupled channels for quasi-elastic scattering of determining diffuseness parameters in Woods-Saxon potential for nuclear reaction. In AIP Conference Proceedings (Vol. 2414, No. 1). AIP Publishing.

[22] Hagino, K., & Takigawa, N. (2012). Subbarrier fusion reactions and many-particle quantum tunneling. Progress of theoretical physics, 128(6), 1061-1106.

[23] Tarbool, Q. J., & Jassim, K. S. (2015). A Study of the surface diffuseness of inter-nucleus potential with quasi-elastic scattering for the 32, 3416S+ 208. Al-Bahir Journal for Engineering and Pure Sciences, 1(1, 2).

[24] Evers, M., Dasgupta, M., Hinde, D. J., Gasques, L. R., Brown, M. L., Rafiei, R., & Thomas, R. G. (2008). Systematic study of the nuclear potential diffuseness through high precision back-angle quasi-elastic scattering. Physical Review C, 78(3), 034614.